

## Supporting Information

# Shape-controlled synthesis of $\text{Co}_3\text{O}_4$ for enhanced electrocatalysis of the oxygen evolution reaction

Boopathi Sidhureddy, Jesse S. Dondapati and Aicheng Chen\*

Electrochemical Technology Centre, Department of Chemistry, University of Guelph

50 Stone Road East, Guelph, ON N1G 2W1, Canada

\*Corresponding Author. Email: aicheng@uoguelph.ca

## Experimental Section

### Materials

Analytical-grade  $\text{Co}(\text{NO}_3)_2$ ,  $\text{NaOH}$ , and  $\text{NaBH}_4$  were procured from Sigma Aldrich. All solutions were prepared in pure water with a conductivity of  $18.2 \text{ M}\Omega\cdot\text{cm}$  (NANOpure Diamond UV ultrapure water purification system).

### Synthesis of shape-controlled $\text{Co}_3\text{O}_4$

For the synthesis of  $\text{Co}_3\text{O}_4$  rods, 10 mL of 0.10 M  $\text{Co}(\text{NO}_3)_2$  was mixed with 10 mL of 0.20 M of  $\text{NaOH}$ . The mixture was then transferred to a Teflon container and placed in a stainless steel hydrothermal setup. The hydrothermal setup was heated to  $180 \text{ }^\circ\text{C}$  at the rate of  $10 \text{ }^\circ\text{C min}^{-1}$  and the temperature was maintained for 4 h and allowed to cool naturally. The synthesis product was thoroughly rinsed using a water/ethanol mixture. A brown colored solid product was obtained and dried in an air oven overnight. The brown colored solid product was finely ground and placed in a muffle furnace. Finally, the product was calcinated at  $450 \text{ }^\circ\text{C}$  for 4 h to obtain the  $\text{Co}_3\text{O}_4$  rods. In

the case of the  $\text{Co}_3\text{O}_4$  cubes, a similar synthetic protocol was followed with some modifications. Briefly, 0.2 M of  $\text{Co}(\text{NO}_3)_2$  and 0.05 M of NaOH were taken in the hydrothermal process. For the synthesis of the  $\text{Co}_3\text{O}_4$  sheets, a chemical reduction and a subsequent calcination procedure were carried out for the formation of 2D sheets. Firstly, 4 mM  $\text{Co}(\text{NO}_3)_2$  was reduced under vigorous stirring condition using aqueous  $\text{NaBH}_4$  solutions (0.1 g/10 mL). The reduced product was collected by centrifugation and rinsed thoroughly with water/ethanol mixture and dried at 70 °C. Secondly, the reduced product was annealed at 450 °C for 4 hr.

### **Surface Characterization**

A field-emission scanning electron microscope (Hitachi SU-70) was employed to characterize the morphology of the synthesized cobalt oxides. X-ray diffraction studies were conducted using a Pananalytical Xpert Pro Diffractometer with Ni filtered monochromatic Cu K $\alpha$  (1.5406 Å, 2.2 KW Max). X-ray photoelectron spectroscopic analysis was performed using an Omicron XPS system, where the size of the X-ray spot was 400  $\mu\text{m}$  using an Al K $\alpha$  monochromatic source. Transmission electron microscopic images were recorded using a JEOL 2010F TEM with a resolution of 0.23 nm.

### **Preparation of electrodes and electrocatalytic study**

A 4.0 mg sample of  $\text{Co}_3\text{O}_4$  rods,  $\text{Co}_3\text{O}_4$  sheets, or  $\text{Co}_3\text{O}_4$  cubes was added to a mixture of 950  $\mu\text{l}$   $\text{H}_2\text{O}$  and 50  $\mu\text{l}$  of Nafion (10 wt.%, Sigma Aldrich). The mixture was sonicated for 30 min. after which aliquots of these inks were cast on a pre-cleaned glassy carbon electrode (CH instruments Inc.; diameter 3.0 mm), and finally the drop-cast electrode was dried at room temperature for 30 min. For the long term stability test, a nickel foam (0.5  $\text{cm}^2$ ) electrode was used in which the

catalyst ink was drop-coated with a mass loading of 0.5 mg cm<sup>-2</sup>. The catalyst coated nickel foam was dried naturally and then treated at 200 °C under an argon atmosphere for the better adherence of the catalyst with the Ni foam. A CH Electrochemical work station (CHI 660E) was employed for all the electrochemical measurements. Cyclic voltammetry (CV), linear sweep voltammetry (LSV), chronopotentiometry (E-t), electrochemical impedance spectroscopic (EIS) analyses were performed in a 1 M KOH solution. Ag/AgCl (3M KCl) and a graphite rod were used as reference and counter electrodes, respectively. The electrochemical data has been normalized with the geometrical areas (GCE 0.07 cm<sup>2</sup> and Ni foam 0.5 cm<sup>2</sup>). The oxygen evolution onset potential was measured by drawing tangent lines manually on the LSV curves, where the intersection point at the x-axis was considered as the onset potential. For comparison, the reference electrode potential was converted to a reversible hydrogen electrode (RHE) using the following Equation 1.

$$E_{RHE} = E_{Ag/AgCl} + 0.059 pH + 0.197 \quad Eq(1)$$

The exchange current density ( $j_o$ , A cm<sup>-2</sup>) was one of the kinetic parameters that was calculated from the EIS using the equation 2.

$$j_o = \frac{RT}{nFAR_{ct}} \quad Eq(2)$$

Where, R, T, n, F, A, and R<sub>ct</sub> are the gas constant, temperature, number electrons, Faraday constant, electrode area, and charge transfer resistant, respectively. Further, the turnover frequency for the OER reaction was calculated using equation 3.

$$TOF = \frac{I N_A}{nN_{surf}F} \quad Eq(3)$$

where I is the measured current at 1.60 V; N<sub>A</sub>, N<sub>surf</sub>, n, and F are Avogadro number, number Co active sites, number of electrons involved in the OER, Faraday constant, respectively. From Fig.

4A, the  $N_{\text{surf}}$  was calculated based on the oxidation peak charge for the formation of Co(III) to Co(IV).

### **Computational Studies**

The DFT total energy optimization for all structures was carried out using generalized gradient approximation (GGA) with parameters of Perdew, Burke, and Ernzerhof (PBE) of CASTEP. As illustrated in Fig. S4, a unit cell of the  $\text{Co}_3\text{O}_4$  spinel structure was drawn to represent the 3D nanocubes, while a layered structure was drawn to represent the 2D nanosheets using GaussView v6.0.16 software. The HOMO-LUMO energy gap for the 2D  $\text{Co}_3\text{O}_4$  was calculated using molecular orbitals tool and Hatree-Fock method with 321-G basis set using Guassian 16W software to be 1.69 eV. The band gap of the 3D structure was found to be 1.9 eV, which is consistent with the value reported in the literature.<sup>1</sup>

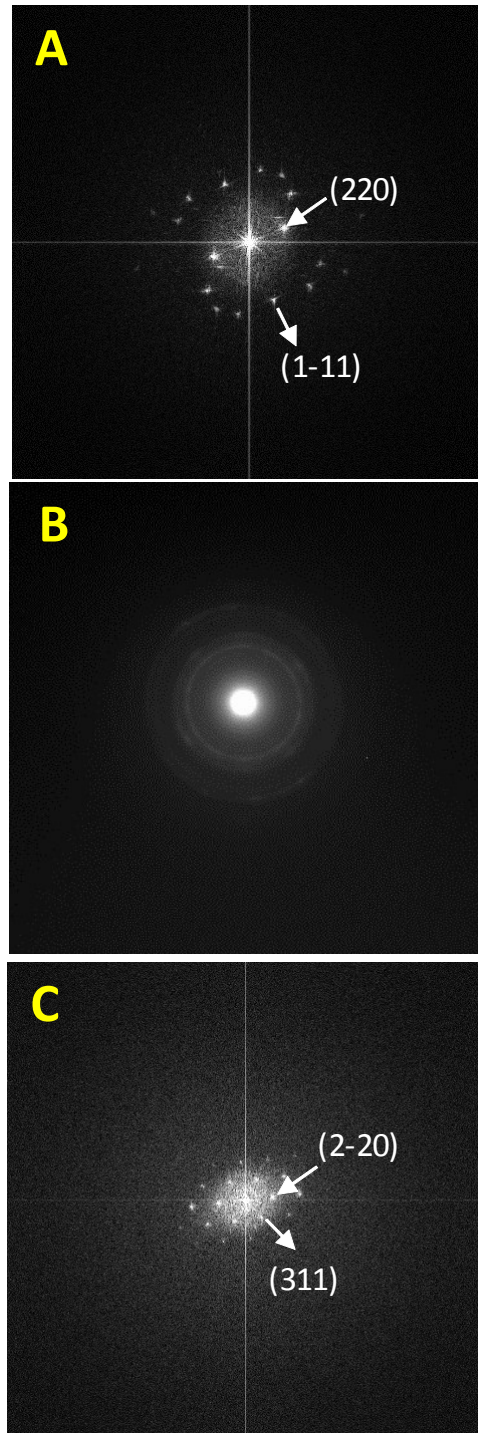


Fig. S1 Selected area diffraction pattern of 1D rods, 2D sheets, and 3D cube-shaped  $\text{Co}_3\text{O}_4$ .

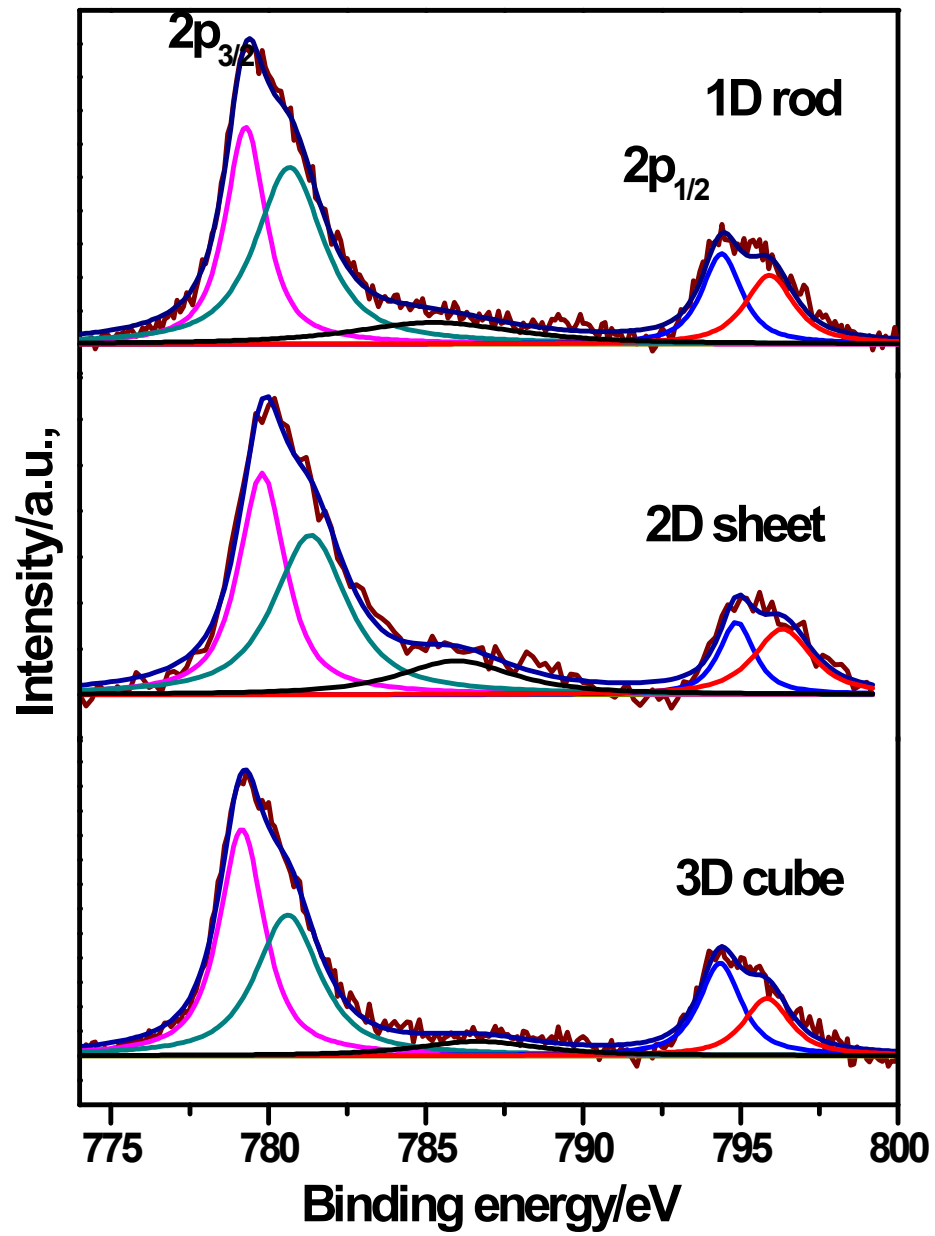


Fig. S2 Co 2p XPS spectra of 1D rods, 2D sheets, and 3D cube-shaped Co<sub>3</sub>O<sub>4</sub>.

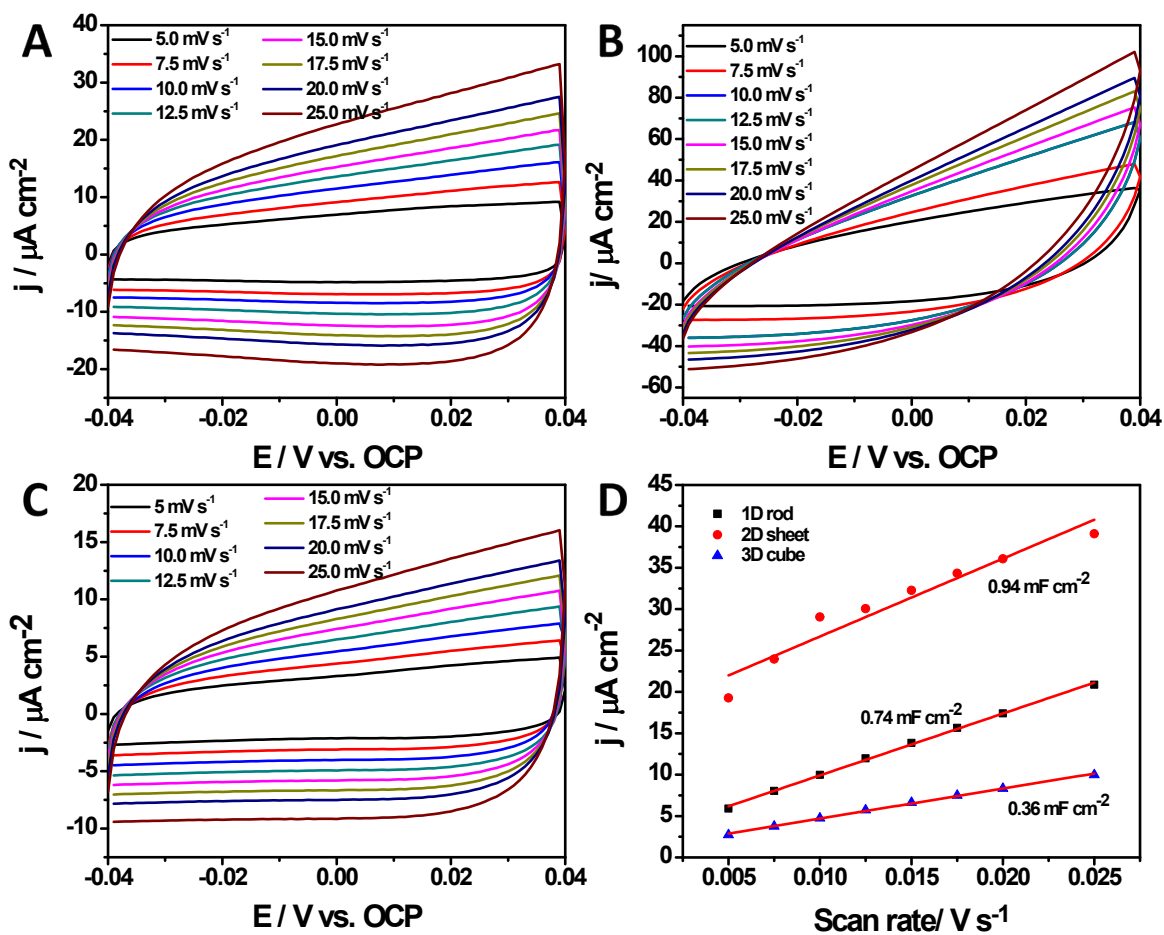


Fig. S3 A-C) CVs of differently shaped  $\text{Co}_3\text{O}_4$ : A) 1D rods, B) 2D sheets, and C) 3D cubes. D) Plots of the current density measured at 0.0 V vs the scan rate to determine the double-layer capacitance.

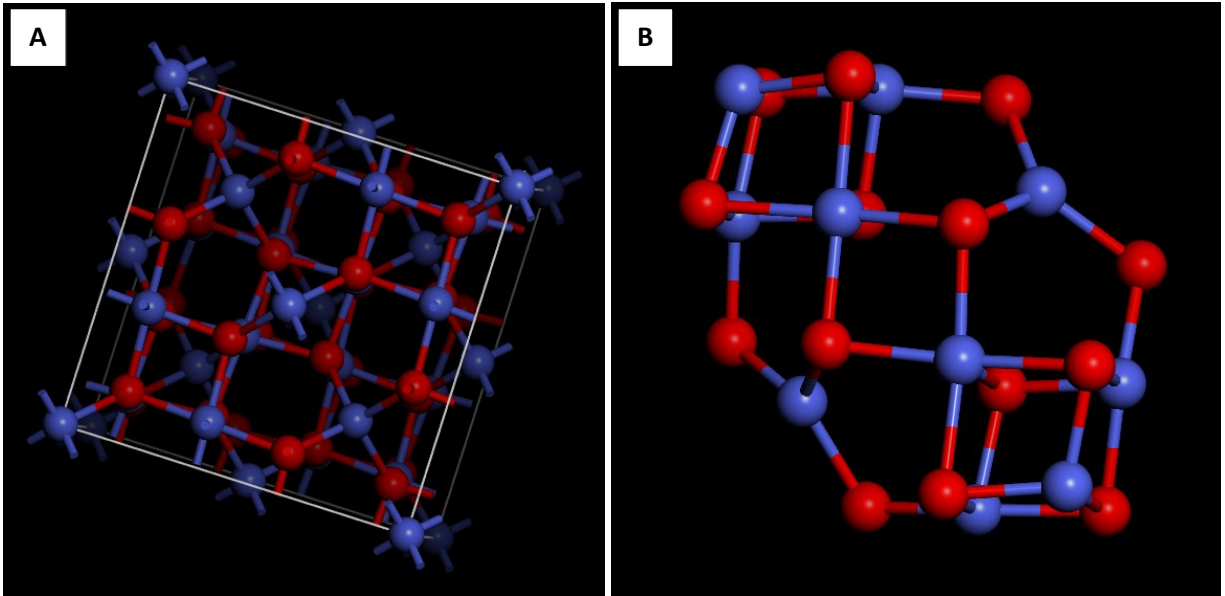


Fig. S4 (A) The  $\text{Co}_3\text{O}_4$  spinel structure unit cell; (B) the  $\text{Co}_3\text{O}_4$  layered structure.



Table S1. EIS data obtained by fitting the Nyquist plots of Fig. 3B.

Catalyst	R <sub>p</sub> (ohm cm <sup>2</sup> )	R <sub>ct</sub> (ohm cm <sup>2</sup> )	CPE -T (mF cm <sup>-2</sup> )	CPE -T	j <sub>o</sub> (mA cm <sup>-2</sup> )
1D rod	0.70	9.80	4.10	0.91	0.656
2D sheet	1.40	3.15	16.9	0.86	2.040
3D cube	1.41	13.86	1.13	0.91	0.464

Table S2. Comparison of the OER performance of Co<sub>3</sub>O<sub>4</sub>-2D sheet with the recent reported electrocatalysts.

Catalyst	Electrolyte	E/V vs. RHE @ 10.0 mA cm <sup>-2</sup>	Reference
Co <sub>3</sub> O <sub>4</sub> - nanooctahedra	0.1 M KOH	1.780	2
Co <sub>3</sub> O <sub>4</sub> – Thin film	1 M NaOH	1.607	3
Mesoporus Pd-Co <sub>3</sub> O <sub>4</sub>	0.1 M KOH	1.680	4
Mesoporous Co <sub>3</sub> O <sub>4</sub>	1 M KOH	1.610	5
Ultrathin Co <sub>3</sub> O <sub>4</sub>	1 M KOH	1.620	6
Ag doped Co <sub>3</sub> O <sub>4</sub> nanosheet	0.5 M H <sub>2</sub> SO <sub>4</sub>	1.700	7
rGo-Co <sub>3</sub> O <sub>4</sub> -yolk-shell nanocages	0.1 M KOH	1.640	8
Co <sub>3</sub> O <sub>4</sub> nanoparticles	1 M KOH	1.619	9
c-Co <sub>3</sub> O <sub>4</sub>	0.1 M KOH	1.726	10
Co <sub>3</sub> O <sub>4</sub> -2D sheet	1 M KOH	1.604	Present work

## References

- (1) J. Chen and A. Selloni, *Phys. Rev. B*, 2012, **85**, 085306.
- (2) Z. Chen; C. X. Kronawitter; B. E. Koel. *Phys. Chem. Chem. Phys.* 2015, **17**, 29387–29393.
- (3) H. S. Jeon; M. S. Jee; H. Kim; S. J. Ahn; Y. J. Hwang; B. K. Min. *ACS Appl. Mater. Interfaces* 2015, **7**, 24550–24555.
- (4) Q. Qu; J. H. Zhang; J. Wang; Q. Y. Li; C. W. Xu; X. Lu. *Sci. Rep.* 2017, **7**, 41542.
- (5) S. Chen; Y. Zhao; B. Sun; Z. Ao; X. Xie; Y. Wei; G. Wang. *ACS Appl. Mater. Interfaces* 2015, **7**, 3306–3313.
- (6) J. Bao, X. Zhang, B. Fan, J. Zhang, M. Zhou, W. Yang, X. Hu, H. Wang, B. Pan and Y. Xie, *Angew. Chemie - Int. Ed.*, 2015, **54**, 7399–7404.
- (7) K.-L. Yan, J.-F. Qin, J.-H. Lin, B. Dong, J.-Q. Chi, Z.-Z. Liu, F.-N. Dai, Y.-M. Chai and C.-G. Liu, *J. Mater. Chem. A*, 2018, **6**, 5678–5686.
- (8) Z. Wu, L.-P. Sun, M. Yang, L.-H. Huo, H. Zhao and J.-C. Grenier, *J. Mater. Chem. A*, 2016, **4**, 13534–13542.
- (9) S. Gupta, A. Yadav, S. Bhartiya, M. K. Singh, A. Miotello, A. Sarkar and N. Patel, *Nanoscale*, 2018, **10**, 8806–8819.
- (10) X. Deng, W. N. Schmidt and H. Tüysüz, *Chem. Mater.*, 2014, **26**, 6127–6134.